12-2013

The Computation of Fluid Velocity in A Closed Cavity with A Moving Lid

Daniel A. Montez
University of Texas-Pan American

THE COMPUTATION OF FLUID VELOCITY IN A CLOSED CAVITY WITH A MOVING LID

A Thesis

by

DANIEL A. MONTEZ

Submitted to the Graduate School of
The University of Texas-Pan American
In partial fulfillment of the requirements for the degree of

MASTER OF SCIENCE

December 2013

Major Subject: Mathematics

THE COMPUTATION OF FLUID VELOCITY IN A CLOSED CAVITY WITH A MOVING LID

A Thesis
by
DANIEL A. MONTEZ

COMMITTEE MEMBERS

Dr. Dambaru Bhatta
Chair of Committee

Dr. Andras Balogh
Committee Member

Dr. Paul Bracken
Committee Member

Dr. Kenichi Maruno
Committee Member

December 2013

ABSTRACT

Montez, Daniel A., The Computation of Fluid Velocity in a Closed Cavity with a Moving Lid. Master of Science (MS), December, 2013, 35 pp., 3 tables, 22 figures, 7 references, 11 titles.

We consider a cavity filled with fluid whose three sides are stationary and the lid at the top is moving at a constant speed. The flow in the cavity is modeled using the conservation of mass and momentum equations with proper boundary conditions. We compute the fluid velocity for the steady state case using the finite element method. We seek the weak formulation and develop a finite element model based on the Galerkin method. Furthermore we use the penalty function method to modify our weak formulation to eliminate the pressure. The Gaussian quadrature method is used to evaluate our integrals over the elements. We present numerical results for two cases. In the first case we consider a square cavity in shape while in the second case we consider a semi-elliptical bump protruding from the bottom. We present our results in tabular and graphical forms.

DEDICATION

I don't know where I would be without my loving family and wife. Their endless support helped guide me through tough times. My wife, Maria Montez, my mother Betty Montez, my father Daniel Montez, my sisters Itzel and Kristin, my nephews Ian and Aidan Gonzales, I love you guys.

ACKNOWLEDGMENTS

I would like to give a special acknowledgment to my advisor Dr. Dambaru Bhatta. I'd like to thank him for his motivation and infinite patience with me.

TABLE OF CONTENTS

Page

LIST OF TABLES

Page

LIST OF FIGURES

Page

CHAPTER I

INTRODUCTION

Fluid mechanics describes the motion of liquids and gases while giving us insight into how they interact with their surroundings. For example, a blue whale moving through the water or how brake fluid is involved in stopping a vehicle. In the same vein fluid mechanics can help us build boats or cars with better braking ability. Intermolecular forces are what bond molecules together. Solids possess very strong intermolecular forces while the forces that hold fluids together are relatively weak. The weak bonds can be illustrated by how a fluid like water is easily deformed.

The properties that a fluid displays allows us to categorize the different types of flows. Viscosity describes a fluids resistance to flow. Inviscid fluids generally have a viscosity of zero. The more resistant a fluid is the higher it's viscosity and vise versa. A natural example of an inviscid fluid would be water while a fluid with a high viscosity would exhibit properties normally found in substances like oil, lard, and honey. The compressibility of a fluid is another way of categorizing flows. The air that we breathe is highly compressible while brake fluid by design is incompressible. Ideal fluids are those that are both incompressible and inviscid. Real fluids usually have some viscosity and might be compressible or not. Furthermore if a fluid displays a linear stress and strain relationship we can call the fluid Newtonian otherwise it is simply non-Newtonian.

If a given viscous fluid is unstable we say the fluid is turbulent. To help illustrate this consider the flow of blood moving through an artery. On the other side if a fluid is relatively smooth in its movement's we say the fluid is laminar. Laminar fluid can be visualized as the calm waters of a lake or other body of water. When discussing viscous flows we introduce a parameter called the Reynolds number. This number defined by $Re = \rho UL/\mu$, where ρ is the density, μ the

fluid viscosity, U the flow velocity, and L the characteristic dimension of the flow region. (Reddy 2005)

The finite element method is a tool to solve partial differential equations. The finite elment is used widely in engineering one of it's many applications is the fatigue analysis of structures. We'll obtain our results using the finite element method which holds many advantages to other numerical methods in that it allows for more complex domains then say the finite difference method. The other advantage that it holds is that we can we can approximate solutions to a subdomain using interpolating polynomials. These finite elements can than be assembled to give us our approximate solution. While there are many upside to the method it should be pointed out that errors can still be introduced at different stages of the method. Take for example trying fit a square inside a circle, the inherit problem with this is that the domains are not an exact match there will be some error introduced there. Error can also accumulate because of the contribution of local matrices which are observed in the global matrix.

CHAPTER II

MATHEMATICAL FORMULATION

Problem Statement

Fluid movement is governed by the laws of conservation of mass, energy and momentum. We present the mass and momentum equations as a set of partial differential equations in Eularian systems. Our dependent variables are the velocity and pressure in this case. For a Newtonian, viscous, incompressible fluid, the equations of conservation of mass and momentum are

$$\nabla \cdot \boldsymbol{v} = 0 \tag{1}$$

$$\rho \left[\frac{\partial \boldsymbol{v}}{\partial t} + \boldsymbol{v} \cdot (\nabla \boldsymbol{v}) \right] = -\nabla P + \mu \nabla^2 \boldsymbol{v} \tag{2}$$

and are satisfied in the fluid domain Ω, where $\boldsymbol{v}$, ρ, P, μ represent the velocity vector, the density, the pressure, and the viscosity respectively. On the boundary $\Gamma = \Gamma_\sigma \cup \Gamma_v$, Dirichlets condition is satisfied on Γ_v and Neumanns conditions is satisfied on Γ_σ. A schematic diagram is shown below.

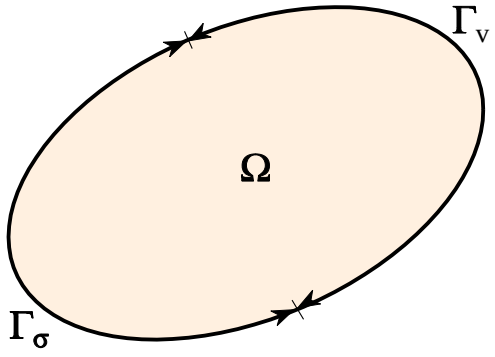

Figure 1: Fluid Domain Ω with Boundary Γ

For our case we'll use Dirichlet condition throughout. We consider the two dimensional steady state case for the current study. The equations (1) and (2) become

$$\frac{\partial v_x}{\partial x} + \frac{\partial v_y}{\partial y} = 0 \tag{3}$$

$$\rho\left(v_x\frac{\partial v_x}{\partial x} + v_y\frac{\partial v_x}{\partial y}\right) - \frac{\partial}{\partial x}\left(2\mu\frac{\partial v_x}{\partial x}\right) - \frac{\partial}{\partial y}\left\{\mu\left(\frac{\partial v_x}{\partial y} + \frac{\partial v_y}{\partial x}\right)\right\} + \frac{\partial P}{\partial x} = 0 \tag{4}$$

$$\rho\left(v_x\frac{\partial v_y}{\partial x} + v_y\frac{\partial v_y}{\partial y}\right) - \frac{\partial}{\partial y}\left(2\mu\frac{\partial v_y}{\partial y}\right) - \frac{\partial}{\partial x}\left\{\mu\left(\frac{\partial v_x}{\partial y} + \frac{\partial v_y}{\partial x}\right)\right\} + \frac{\partial P}{\partial y} = 0 \tag{5}$$

Here v_x and v_y represent x-component and y-component of $\boldsymbol{v}$ respectively, i.e., $\boldsymbol{v} = (v_x,\, v_y)$.

Weak Formulation

To develop the finite element model, first derive the weak formulation of the above equations as follows. We consider an element denoted by Ω^e which is a subdomain of Ω and $\Gamma^e$is the boundary of Ω^e. The weighted integral statements for this typical element are

$$\int_{\Omega^e} w_1\left(\rho\left(v_x\frac{\partial v_x}{\partial x} + v_y\frac{\partial v_x}{\partial y}\right) - \frac{\partial \ell_{xx}}{\partial x} - \frac{\partial \ell_{xy}}{\partial y}\right)dxdy = 0 \tag{6}$$

$$\int_{\Omega^e} w_2\left(\rho\left(v_x\frac{\partial v_y}{\partial x} + v_y\frac{\partial v_y}{\partial y}\right) - \frac{\partial \ell_{xy}}{\partial x} - \frac{\partial \ell_{yy}}{\partial y}\right)dxdy = 0 \tag{7}$$

$$\int_{\Omega^e} Q\left(\frac{\partial v_x}{\partial x} + \frac{\partial v_y}{\partial y}\right)dxdy = 0 \tag{8}$$

where w_1, w_2 and Q are weight functions. Also we use the following notations: $\ell_{xx} = 2\mu\frac{\partial v_x}{\partial x} - P$, $\ell_{xy} = \mu\left(\frac{\partial v_x}{\partial y} + \frac{\partial v_y}{\partial x}\right)$, and $\ell_{yy} = 2\mu\frac{\partial v_y}{\partial y} - P$.

We trade the differentiation with the aid of the following equations

$$\begin{aligned}
\frac{\partial}{\partial x}(w_1\ell_{xx}) &= \frac{\partial w_1}{\partial x}\ell_{xx} + w_1\frac{\partial \ell_{xx}}{\partial x} \\
\oint_{\Gamma^e} n_x w_1 \ell_{xx} ds &= \int_{\Omega^e}\left(\frac{\partial w_1}{\partial x}\ell_{xx} + w_1\frac{\partial \ell_{xx}}{\partial x}\right) dxdy \\
-\int_{\Omega^e} w_1\frac{\partial \ell_{xx}}{\partial x} dxdy &= \int_{\Omega^e}\frac{\partial w_1}{\partial x}\ell_{xx} dxdy - \oint_{\Gamma^e} n_x w_1 \ell_{xx} ds
\end{aligned} \tag{9}$$

Here n_x denotes the x-component of the normal to the boundary.

Similarly, we have

$$\begin{aligned}
\frac{\partial}{\partial y}(w_1\ell_{xy}) &= \frac{\partial w_1}{\partial y}\ell_{xy} + w_1\frac{\partial \ell_{xy}}{\partial y} \\
\oint_{\Gamma^e} n_y w_1 \ell_{xy} ds &= \int_{\Omega^e}\left(\frac{\partial w_1}{\partial y}\ell_{xy} + w_1\frac{\partial \ell_{xy}}{\partial y}\right) dxdy \\
-\int_{\Omega^e} w_1\frac{\partial \ell_{xy}}{\partial y} dxdy &= \int_{\Omega^e}\frac{\partial w_1}{\partial y}\ell_{xy} dxdy - \oint_{\Gamma^e} n_y w_1 \ell_{xy} ds
\end{aligned} \tag{10}$$

with n_y denotes the y-component of the normal to the boundary.

$$\begin{aligned}
\frac{\partial}{\partial x}(w_2\ell_{yy}) &= \frac{\partial w_2}{\partial y}\ell_{yy} + w_2\frac{\partial \ell_{yy}}{\partial y} \\
\oint_{\Gamma^e} n_y w_2 \ell_{yy} ds &= \int_{\Omega^e}\left(\frac{\partial w_2}{\partial y}\ell_{yy} + w_2\frac{\partial \ell_{yy}}{\partial y}\right) dxdy \\
-\int_{\Omega^e} w_2\frac{\partial \ell_{yy}}{\partial y} dxdy &= \int_{\Omega^e}\frac{\partial w_2}{\partial y}\ell_{yy} dxdy - \oint_{\Gamma^e} n_y w_2 \ell_{yy} ds
\end{aligned} \tag{11}$$

and, finally

$$\begin{aligned}
\frac{\partial}{\partial x}(w_2\ell_{xy}) &= \frac{\partial w_2}{\partial x}\ell_{xy} + w_2\frac{\partial \ell_{xy}}{\partial x} \\
\oint_{\Gamma^e} n_x w_2 \ell_{xy} ds &= \int_{\Omega^e}\left(\frac{\partial w_2}{\partial x}\ell_{xy} + w_2\frac{\partial \ell_{xy}}{\partial x}\right) dxdy \\
-\int_{\Omega^e} w_2\frac{\partial \ell_{xy}}{\partial x} dxdy &= \int_{\Omega^e}\frac{\partial w_2}{\partial x}\ell_{xy} dxdy - \oint_{\Gamma^e} n_x w_2 \ell_{xy} ds
\end{aligned} \tag{12}$$

We substitute (9), (10), (11), and (12) into the appropriate weighted integral statements (6), (7), and (8). The final expressions are

$$\int_{\Omega^e}\left[w_1\rho\left(v_x\frac{\partial v_x}{\partial x}+v_y\frac{\partial v_x}{\partial y}\right)+\frac{\partial w_1}{\partial x}\left(2\mu\frac{\partial v_x}{\partial x}-P\right)+\frac{\partial w_1}{\partial y}\left\{\mu\left(\frac{\partial v_x}{\partial y}+\frac{\partial v_y}{\partial x}\right)\right\}\right]dxdy$$
$$-\oint_{\Gamma^e} w_1\left[n_x\left(2\mu\frac{\partial v_x}{\partial x}-P\right)ds+n_y\left\{\mu\left(\frac{\partial v_x}{\partial y}+\frac{\partial v_y}{\partial x}\right)\right\}\right]ds=0 \tag{13}$$

$$\int_{\Omega^e}\left[w_2\rho\left(v_x\frac{\partial v_y}{\partial x}+v_y\frac{\partial v_y}{\partial y}\right)+\frac{\partial w_2}{\partial x}\left\{\mu\left(\frac{\partial v_x}{\partial y}+\frac{\partial v_y}{\partial x}\right)\right\}+\frac{\partial w_2}{\partial y}\left(2\mu\frac{\partial v_y}{\partial y}-P\right)\right]dxdy$$
$$-\oint_{\Gamma^e} w_2\left[n_x\left\{\mu\left(\frac{\partial v_x}{\partial y}+\frac{\partial v_y}{\partial x}\right)\right\}ds+n_y\left(2\mu\frac{\partial v_y}{\partial y}-P\right)\right]ds=0 \tag{14}$$

$$\int_{\Omega^e} Q\left(\frac{\partial v_x}{\partial x}+\frac{\partial v_y}{\partial y}\right)dxdy=0 \tag{15}$$

We proceed by developing the Galerkin finite element model. We express the velocity components and pressure as follows

$$v_x(x,y)=\sum_{j=1}^{n}v_x^j\psi_j^e(x,y),\qquad v_y(x,y)=\sum_{j=1}^{n}v_y^j\psi_j^e(x,y)\qquad P=\sum_{J=1}^{m}P_J\phi_j^e(x,y) \tag{16}$$

Here v_x^j, v_y^j and P_J represent our nodal values while$\psi_j^e(x,y)$ and $\phi_j^e(x,y)$ are our shape functions. Discussion on shape functions is presented later. Using the expressions (16) into the equations (13), (14), (15), we obtain

$$\int_{\Omega^e} w_1\rho\left(v_x\frac{\partial}{\partial x}\sum_{j=1}^{n}v_x^j\psi_j^e+v_y\frac{\partial}{\partial y}\sum_{j=1}^{n}v_x^j\psi_j^e\right)+\frac{\partial w_1}{\partial x}\left\{2\mu\frac{\partial}{\partial x}\left(\sum_{j=1}^{n}v_x^j\psi_j^e\right)-\sum_{J=1}^{m}P_J\phi_j^e\right\}$$
$$+\frac{\partial w_1}{\partial y}\left[\mu\left\{\frac{\partial}{\partial y}\left(\sum_{j=1}^{n}v_x^j\psi_j^e\right)+\frac{\partial}{\partial x}\left(\sum_{j=1}^{n}v_y^j\psi_j^e\right)\right\}\right]=0$$

$$\int_{\Omega^e} w_2\rho\left(v_x\frac{\partial}{\partial x}\sum_{j=1}^{n}v_y^j\psi_j^e+v_y\frac{\partial}{\partial y}\sum_{j=1}^{n}v_y^j\psi_j^e\right)+\frac{\partial w_2}{\partial y}\left\{2\mu\frac{\partial}{\partial y}\left(\sum_{j=1}^{n}v_y^j\psi_j^e\right)-\sum_{J=1}^{m}P_J\phi_j^e\right\}$$
$$+\frac{\partial w_2}{\partial x}\left[\mu\left\{\frac{\partial}{\partial y}\left(\sum_{j=1}^{n}v_x^j\psi_j^e\right)+\frac{\partial}{\partial x}\left(\sum_{j=1}^{n}v_y^j\psi_j^e\right)\right\}\right]=0$$

$$\int_{\Omega^e} Q\left\{\frac{\partial}{\partial x}\left(\sum_{j=1}^{n}v_x^j\psi_j^e\right)+\frac{\partial}{\partial y}\left(\sum_{j=1}^{n}v_y^j\psi_j^e\right)\right\}dxdy=0$$

Note that since we are using the Galerkin method we have that $w_1 \approx v_x,\ w_2 \approx v_y,\ and\ Q \approx P.$

So after simplification, we have

$$\int_{\Omega^e} \left[\rho \psi_i^e \left(v_x \frac{\partial \psi_j^e}{\partial x} + v_y \frac{\partial \psi_j^e}{\partial y} \right) v_x^j + \mu \frac{\partial \psi_i^e}{\partial y} \frac{\partial \psi_j^e}{\partial y} v_x^j + \mu \frac{\partial \psi_i^e}{\partial y} \frac{\partial \psi_i^e}{\partial x} v_y^j + 2\mu \frac{\partial \psi_i^e}{\partial x} \frac{\partial \psi_j^e}{\partial x} v_x^j - \frac{\partial \psi_i^e}{\partial x} \phi_j^e P_J \right] dxdy = 0 \tag{17}$$

$$\int_{\Omega^e} \left[\rho \psi_i^e \left(v_x \frac{\partial \psi_j^e}{\partial x} + v_y \frac{\partial \psi_j^e}{\partial y} \right) v_y^j + \mu \frac{\partial \psi_i^e}{\partial x} \frac{\partial \psi_j^e}{\partial y} v_x^j + \mu \frac{\partial \psi_i^e}{\partial x} \frac{\partial \psi_j^e}{\partial x} v_y^j + 2\mu \frac{\partial \psi_i^e}{\partial y} \frac{\partial \psi_j^e}{\partial y} v_y^j - \frac{\partial \psi_i^e}{\partial y} \phi_j^e P_J \right] dxdy = 0 \tag{18}$$

$$- \int_{\Omega^e} \left[\psi_i^e \frac{\partial \psi_j^e}{\partial x} v_x^j + \psi_i^e \frac{\partial \psi_j^e}{\partial y} v_y^j \right] dxdy = 0 \tag{19}$$

We can write this in matrix form as

$$\begin{bmatrix} N(\boldsymbol{v}) & 0 & 0 \\ 0 & N(\boldsymbol{v}) & 0 \\ 0 & 0 & 0 \end{bmatrix} \begin{bmatrix} v_x \\ v_y \\ P \end{bmatrix} + \begin{bmatrix} M_{11} & M_{12} & M_{13} \\ M_{21} & M_{22} & M_{23} \\ M_{31} & M_{32} & M_{33} \end{bmatrix} \begin{bmatrix} v_x \\ v_y \\ P \end{bmatrix} = \begin{bmatrix} F^{(1)} \\ F^{(2)} \\ 0 \end{bmatrix} \tag{20}$$

where

$$
\begin{aligned}
N(\boldsymbol{v}) &= \int_{\Omega^e} \rho\psi_i^e \left(v_x \frac{\partial \psi_j^e}{\partial x} + v_y \frac{\partial \psi_j^e}{\partial y} \right) dxdy \\
M_{11} &= \int_{\Omega^e} \mu \left[2\frac{\partial \psi_i^e}{\partial x}\frac{\partial \psi_j^e}{\partial x} + \frac{\partial \psi_i^e}{\partial y}\frac{\partial \psi_j^e}{\partial y} \right] dxdy \\
M_{12} &= \int_{\Omega^e} \mu \frac{\partial \psi_i^e}{\partial y}\frac{\partial \psi_i^e}{\partial x}\, dxdy \\
M_{13} &= -\int_{\Omega^e} \frac{\partial \psi_i^e}{\partial x}\phi_j^e\, dxdy \\
M_{21} &= -\int_{\Omega^e} \mu \frac{\partial \psi_i^e}{\partial x}\frac{\partial \psi_j^e}{\partial y}\, dxdy \\
M_{22} &= \int_{\Omega^e} \mu \left[\frac{\partial \psi_i^e}{\partial x}\frac{\partial \psi_j^e}{\partial x} + 2\frac{\partial \psi_i^e}{\partial y}\frac{\partial \psi_j^e}{\partial y} \right] dxdy \\
M_{23} &= -\int_{\Omega^e} \frac{\partial \psi_i^e}{\partial y}\phi_j^e\, dxdy \\
M_{31} &= -\int_{\Omega^e} \psi_i^e \frac{\partial \psi_j^e}{\partial x} dxdy \\
M_{32} &= -\int_{\Omega^e} \psi_i^e \frac{\partial \psi_j^e}{\partial y} dxdy \\
M_{33} &= 0 \\
F^{(1)} &= \oint_{\Gamma^e} \psi_i^e \left[n_x \left(2\mu \frac{\partial \psi_i^e}{\partial x} - P \right) ds + n_y \left\{ \mu \left(\frac{\partial \psi_i^e}{\partial y} + \frac{\partial \psi_i^e}{\partial x} \right) \right\} \right] ds \\
F^{(2)} &= \oint_{\Gamma^e} \psi_i^e \left[n_y \left(2\mu \frac{\partial \psi_i^e}{\partial y} - P \right) ds + n_x \left\{ \mu \left(\frac{\partial \psi_i^e}{\partial y} + \frac{\partial \psi_i^e}{\partial x} \right) \right\} \right] ds
\end{aligned}
\tag{21}
$$

This is the element level formulation of the governing equations in 2 dimension for our problem.

Quadrilateral Elements and the Gaussian Quadrature

In our study we use 2-dimensional quadrilateral elements. Our interpolation functions in the transformed domain (ξ, η) are

$$\begin{aligned} \psi_1^e(\xi,\,\eta) &= \frac{1}{4}(1-\xi)(1-\eta) \\ \psi_2^e(\xi,\,\eta) &= \frac{1}{4}(1+\xi)(1-\eta) \\ \psi_3^e(\xi,\,\eta) &= \frac{1}{4}(1+\xi)(1+\eta) \\ \psi_4^e(\xi,\,\eta) &= \frac{1}{4}(1-\xi)(1+\eta) \end{aligned} \tag{22}$$

where $-1 \leq (\xi, \eta) \leq 1$. The transformation between the (x, y) domain and (ξ, η) domain is given by

$$\begin{aligned} x &= \sum_{j=1}^{m} x_j^e \psi_j^e(\xi, \eta) \\ y &= \sum_{j=1}^{m} y_j^e \psi_j^e(\xi, \eta) \end{aligned}$$

Furthermore to transform expression in the integrand of our finite element model we use the following relations obtained from the chain rule

$$\begin{aligned} \frac{\partial \psi_i^e}{\partial \xi} &= \frac{\partial \psi_i^e}{\partial x}\frac{\partial x}{\partial \xi} + \frac{\partial \psi_i^e}{\partial y}\frac{\partial y}{\partial \xi} \\ \frac{\partial \psi_i^e}{\partial \eta} &= \frac{\partial \psi_i^e}{\partial x}\frac{\partial x}{\partial \eta} + \frac{\partial \psi_i^e}{\partial y}\frac{\partial y}{\partial \eta} \end{aligned}$$

written in matrix notation we have

$$\begin{bmatrix} \frac{\partial \psi_i^e}{\partial \xi} \\ \frac{\partial \psi_i^e}{\partial \eta} \end{bmatrix} = J \begin{bmatrix} \frac{\partial \psi_i^e}{\partial x} \\ \frac{\partial \psi_i^e}{\partial y} \end{bmatrix}$$

where

$$J = \begin{bmatrix} \frac{\partial x}{\partial \xi} & \frac{\partial y}{\partial \xi} \\ \frac{\partial x}{\partial \eta} & \frac{\partial y}{\partial \eta} \end{bmatrix}$$

is the jacobian matrix. Finally to relate $\frac{\partial \psi_i^e}{\partial x}$ and $\frac{\partial \psi_i^e}{\partial y}$ to $\frac{\partial \psi_i^e}{\partial \xi}$ and $\frac{\partial \psi_i^e}{\partial \eta}$ we are going to need to invert our jacobian matrix to obtain

$$J^{-1} \begin{bmatrix} \frac{\partial \psi_i^e}{\partial \xi} \\ \frac{\partial \psi_i^e}{\partial \eta} \end{bmatrix} = \begin{bmatrix} \frac{\partial \psi_i^e}{\partial x} \\ \frac{\partial \psi_i^e}{\partial y} \end{bmatrix}.$$

To evaluate the expressions in the jacobian we use the coordinate transformations

$$\begin{aligned} \frac{\partial x}{\partial \xi} &= \sum_{j=1}^{m} x_j^e \frac{\partial \psi_j^e}{\partial \xi} \\ \frac{\partial y}{\partial \xi} &= \sum_{j=1}^{m} y_j^e \frac{\partial \psi_j^e}{\partial \xi} \\ \frac{\partial x}{\partial \eta} &= \sum_{j=1}^{m} x_j^e \frac{\partial \psi_j^e}{\partial \eta} \\ \frac{\partial y}{\partial \eta} &= \sum_{j=1}^{m} y_j^e \frac{\partial \psi_j^e}{\partial \eta} \end{aligned}$$

so thus the terms inside of our jacobian can be expressed

$$\begin{bmatrix} \frac{\partial x}{\partial \xi} & \frac{\partial y}{\partial \xi} \\ \frac{\partial x}{\partial \eta} & \frac{\partial y}{\partial \eta} \end{bmatrix} = \begin{bmatrix} \sum_{j=1}^{m} x_j^e \frac{\partial \psi_j^e}{\partial \xi} & \sum_{j=1}^{m} y_j^e \frac{\partial \psi_j^e}{\partial \xi} \\ \sum_{j=1}^{m} x_j^e \frac{\partial \psi_j^e}{\partial \eta} & \sum_{j=1}^{m} y_j^e \frac{\partial \psi_j^e}{\partial \eta} \end{bmatrix}.$$

Also note that $dxdy = Jd\xi d\eta$ Now to actually integrate once we have done our transformation we need to use the following formula

$$\int_{-1}^{1}\int_{-1}^{1} F(\xi,\eta)d\eta d\xi \approx \sum_{I=1}^{M}\sum_{J=1}^{N} F(\xi_I,\eta_J)w_I w_J$$

let M and N denote the number of quadrature points, and let $\xi_I \; and \; \eta_J$ be our Gauss points that we will be using while w_I and w_J are called the Gauss weights. These Gauss points and weights are very standard as you can see from the table below. (Reddy 2005)

N_g	Points		Weights $(w_I,\ w_J)$
1	$(0.00,\ \ 0.00)$	$1\ pt$	$(2.00,\ 2.00)$
2	$(\pm 0.5773,\ \pm 0.5773)$	$4\ pts$	$(1.00,\ 1.00)$
3	$(\pm 0.7746,\ \pm 0.7746)$ $(0.0,\ 0.0)$ $(\pm 0.7746,\ 0.0)$ $(0.0,\ \pm 0.7746)$	$9\ pts$	$(0.5556,\ 0.5556)$ $(0.8889,\ 0.8889)$ $(0.5556,\ 0.8889)$ $(0.8889,\ 0.5556)$
4	$(\pm 0.3399,\ \pm 0.3399)$ $(\pm 0.3399,\ \pm 0.8611)$ $(\pm 0.8611,\ \pm 0.3399)$ $(\pm 0.8611,\ \pm 0.8611)$	$16\ pts$	$(0.6521,\ 0.6521)$ $(0.6521,\ 0.3478)$ $(0.3478,\ 0.6521)$ $(0.3478,\ 0.3478)$

Table 1: Gauss Points and Weights for Squares

Example of the Penalty Method

In this section, we discuss the penalty method and give a simple example. The idea behind the penalty method is straightforward, and it allows us to reformulate a problem that has constraints as one without constraints. As an example consider minimizing the quadratic function

$$f(x,y) \quad = \quad 4x^2 - 3y^2 + 2xy + 6x - 3y + 5$$

subject to the constraint

$$G(x,y) \quad = 2x + 3y \quad = 0$$

where G(x,y) is our constraint. We want to reformulate the problem as finding the minimum of

the modified function F_p

$$F_p(x,y) \;=\; f(x,y) + \frac{\gamma}{2}[G(x,y)]^2$$

where γ is called the penalty parameter. The solution amounts to solving

$$\begin{aligned} \frac{\partial F_p}{\partial x} &= 0 \\ \frac{\partial F_p}{\partial y} &= 0 \end{aligned}$$

If we take $\gamma \to \infty$ the more accurately the constraint will be satisfied and hence our the solution (which ends up being a function of the penalty parameter (x_γ, y_γ)) will approach the actual solution (x,y). Focusing at the problem at hand our modified functional is

$$F_p(x,y) \;=\; 4x^2 - 3y^2 + 2xy + 6x - 3y + 5 + \frac{\gamma}{2}(2x+3y)^2$$

and

$$\begin{aligned} \frac{\partial F_p}{\partial x} &= 8x + 2y + 6 + 2\gamma(2x+3y) &= 0 \\ \frac{\partial F_p}{\partial y} &= -6y + 2x - 3 + 3\gamma(2x+3y) &= 0 \end{aligned}$$

this yields

$$\begin{aligned} x_\gamma &= \frac{15 - 36\gamma}{-26 + 12\gamma} \\ y_\gamma &= \frac{18 + 24\gamma}{-26 + 12\gamma} \end{aligned}$$

If we take

$$\begin{aligned} \lim_{\gamma\to\infty} x_\gamma &= -3 \\ \lim_{\gamma\to\infty} y_\gamma &= 2 \end{aligned}$$

we see that as $\gamma \to \infty$ that $(x_\gamma, y_\gamma) \to (-3, 2)$. (Reddy 2005)

Penalty Formulation for Our Problem

To construct the penalty model for this problem let's define the bilinear and linear forms as follows

$$B_0(\boldsymbol{w}, \boldsymbol{v}) = \int_{\Omega^e} \mu \left[2\left(\frac{\partial w_1}{\partial x}\frac{\partial v_x}{\partial x} + \frac{\partial w_2}{\partial y}\frac{\partial v_y}{\partial y} \right) + \left(\frac{\partial w_1}{\partial y} + \frac{\partial w_2}{\partial y} \right)\left(\frac{\partial v_x}{\partial y} + \frac{\partial v_y}{\partial x} \right) \right] dxdy$$

$$\ell_0(\boldsymbol{w}) = \oint_{\Gamma^e} (w_1 t_x + w_2 t_y) ds$$

Our bilinear form is symmetric, thus we can find a quadratic functional such that the minimum of it is equivalent to the variational problem. The quadratic functional in this case is

$$I_0(\boldsymbol{v}) = \frac{1}{2} B_0(\boldsymbol{v}, \boldsymbol{v}) - \ell_0(\boldsymbol{v}), \tag{23}$$

subject to the constraint

$$G(\boldsymbol{v}) \equiv \frac{\partial v_x}{\partial x} + \frac{\partial v_y}{\partial y} \tag{24}$$

Modified functional that we wish to minimize is

$$I_P(\boldsymbol{v}) \equiv I_0(\boldsymbol{v}) + \frac{\gamma_e}{2} \int_{\Omega^e} [G(\boldsymbol{v})]^2 \tag{25}$$

the one half is used for convenience while the γ_e is called the penalty parameter. The reason why we are interested in the penalty method is that it allows us to construct our model without the pressure. The pressure can be post computed using $\gamma_e \left(\frac{\partial v_x}{\partial x} + \frac{\partial v_y}{\partial y} \right) = -P$ once $v_x,\ v_y$ are known. After incoporating the nonlinear terms, minimization of 25 yields us a matrix equation (Reddy 2004)

$$\begin{bmatrix} N^e(\boldsymbol{v}) & 0 \\ 0 & N^e(\boldsymbol{v}) \end{bmatrix} \begin{bmatrix} v_x \\ v_y \end{bmatrix} + \begin{bmatrix} K^e_{11} & K^e_{12} \\ K^e_{21} & K^e_{22} \end{bmatrix} \begin{bmatrix} v_x \\ v_y \end{bmatrix} = \begin{bmatrix} F^e_1 \\ F^e_2 \end{bmatrix} \tag{26}$$

where

$$\begin{aligned}
K^e_{11} &= \int_{\Omega^e} \left[(2\mu + \gamma_e) \frac{\partial \psi_i}{\partial x} \frac{\partial \psi^e_j}{\partial x} + \frac{\partial \psi_i}{\partial y} \frac{\partial \psi^e_j}{\partial y} \right] dxdy \\
K^e_{12} &= \int_{\Omega} \left[\mu \frac{\partial \psi_i}{\partial y} \frac{\partial \psi^e_j}{\partial x} + \gamma_e \frac{\partial \psi_i}{\partial x} \frac{\partial \psi^e_j}{\partial y} \right] dxdy \\
K^e_{21} &= \int_{\Omega^e} \left[\mu \frac{\partial \psi_i}{\partial x} \frac{\partial \psi^e_j}{\partial y} + \gamma_e \frac{\partial \psi_i}{\partial y} \frac{\partial \psi^e_j}{\partial x} \right] dxdy \\
K^e_{22} &= \int_{\Omega^e} \left[\mu \frac{\partial \psi_i}{\partial x} \frac{\partial \psi^e_j}{\partial x} + (2\mu + \gamma_e) \frac{\partial \psi_i}{\partial y} \frac{\partial \psi^e_j}{\partial y} \right] dxdy \\
F^e_1 &= \oint_{\Gamma^e} \psi^e_i \left[n_x \left(2\mu \frac{\partial \psi^e_i}{\partial x} - P_i \right) ds + n_y \left\{ \mu \left(\frac{\partial \psi^e_i}{\partial y} + \frac{\partial \psi^e_i}{\partial x} \right) \right\} \right] ds \\
F^e_2 &= \oint_{\Gamma^e} \psi^e_i \left[n_y \left(2\mu \frac{\partial \psi^e_i}{\partial y} - P_i \right) ds + n_x \left\{ \mu \left(\frac{\partial \psi^e_i}{\partial y} + \frac{\partial \psi^e_i}{\partial x} \right) \right\} \right] ds \\
N(\boldsymbol{v}) &= \int_{\Omega^e} \rho \psi^e_i \left(v_x \frac{\partial \psi^e_j}{\partial x} + v_y \frac{\partial \psi^e_j}{\partial y} \right) dxdy
\end{aligned} \tag{27}$$

Descretization of the Domain

Now we'll discuss the descretization of the domain. In the first scenario we have a square cavity of side of length one. First we present the descretization, as we can see there are 320 elements and 357 total nodes. The graph below describes the element numbering system employed. We have 17 global nodes along the x-axis the 18th node restarts 1 at the next level from the beginning. Thus per line we have to a total of 16 elements. The numbering continuous in this fashion all the way to the top to node 357 and element 320. (Reddy 2004)

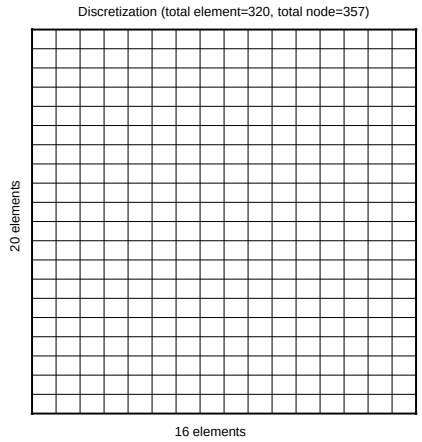

Figure 2: Descretization of a Rectangular Domain

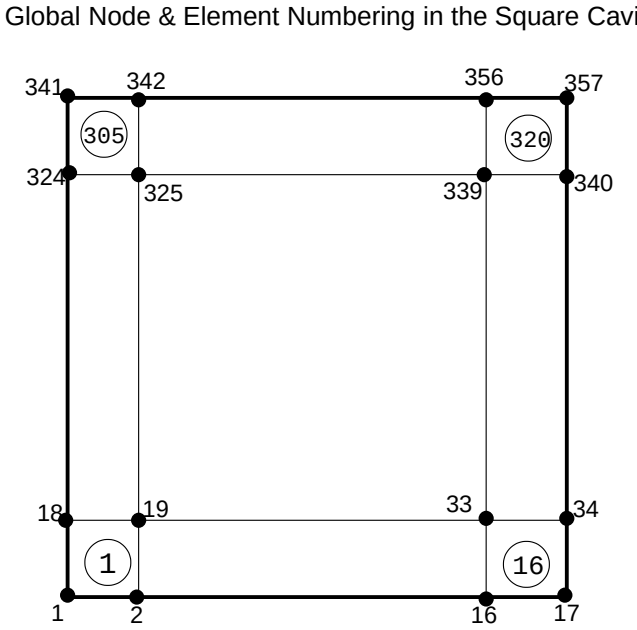

Figure 3: Element and Node Numbering for a Rectangular Domain

Now we descretize our second scenario. We consider a cavity similar to the one described before however in this case the the bottom has a semi-elliptical bump protruding from the bottom up. The descretization has 5 elements and 6 global nodes per line. However in contrast to the previous descretization the numbering resets when we hit the ellipse. In total we see that there are 120 global nodes and 95 elements. The typical numbering scheme will be presented next.

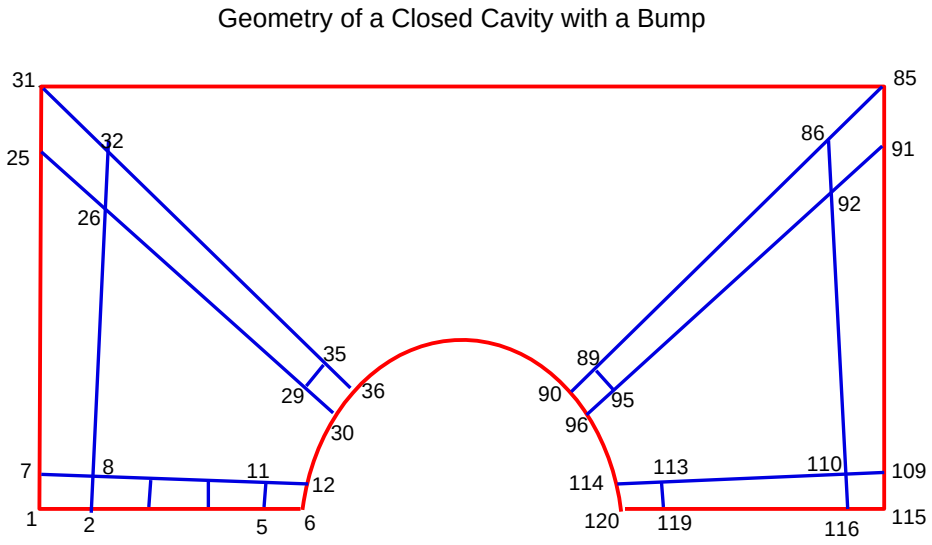

Figure 4: Descretization and Node Numbering for Domain with Semi-Ellipse

The distribution of the global node numberings and the element number is shown below for this particular case

Elem:	Global Nodes	Elem:	Global Nodes
1:	1 2 8 7	2:	2 3 9 8
3:	3 4 10 9	4:	4 5 11 10
5:	5 6 12 11	6:	7 8 14 13
7:	8 9 15 14	8:	9 10 16 15
9:	10 11 17 16	10:	11 12 18 17
11:	13 14 20 19	12:	14 15 21 20
13:	15 16 22 21	14:	16 17 23 22
15:	17 18 24 23	16:	19 20 26 25
17:	20 21 27 26	18:	21 22 28 27
19:	22 23 29 28	20:	23 24 30 29
21:	25 26 32 31	22:	26 27 33 32
23:	27 28 34 33	24:	28 29 35 34
25:	29 30 36 35	26:	31 32 38 37
27:	32 33 39 38	28:	33 34 40 39
29:	34 35 41 40	30:	35 36 42 41
31:	37 38 44 43	32:	38 39 45 44

33: 39 40 46 45
34: 40 41 47 46
35: 41 42 48 47
36: 43 44 50 49
37: 44 45 51 50
38: 45 46 52 51
39: 46 47 53 52
40: 47 48 54 53
41: 49 50 56 55
42: 50 51 57 56
43: 51 52 58 57
44: 52 53 59 58
45: 53 54 60 59
46: 55 56 62 61
47: 56 57 63 62
48: 57 58 64 63
49: 58 59 65 64
50: 59 60 66 65
51: 61 62 68 67
52: 62 63 69 68
53: 63 64 70 69
54: 64 65 71 70
55: 65 66 72 71
56: 67 68 74 73
57: 68 69 75 74
58: 69 70 76 75
59: 70 71 77 76
60: 71 72 78 77
61: 73 74 80 79
62: 74 75 81 80
63: 75 76 82 81
64: 76 77 83 82
65: 77 78 84 83
66: 79 80 86 85
67: 80 81 87 86
68: 81 82 88 87
69: 82 83 89 88
70: 83 84 90 89
71: 85 86 92 91
72: 86 87 93 92
73: 87 88 94 93
74: 88 89 95 94
75: 89 90 96 95
76: 91 92 98 97
77: 92 93 99 98
78: 93 94 100 99
79: 94 95 101 100
80: 95 96 102 101
81: 97 98 104 103
82: 98 99 105 104
83: 99 100 106 105
84: 100 101 107 106
85: 101 102 108 107
86: 103 104 110 109
87: 104 105 111 110
88: 105 106 112 111
89: 106 107 113 112
90: 107 108 114 113
91: 109 110 116 115
92: 110 111 117 116
93: 111 112 118 117
94: 112 113 119 118
95: 113 114 120 119

Finally the descretization for the same scenario as previously discussed ,but in this case with 297 global nodes and with 256 elements.

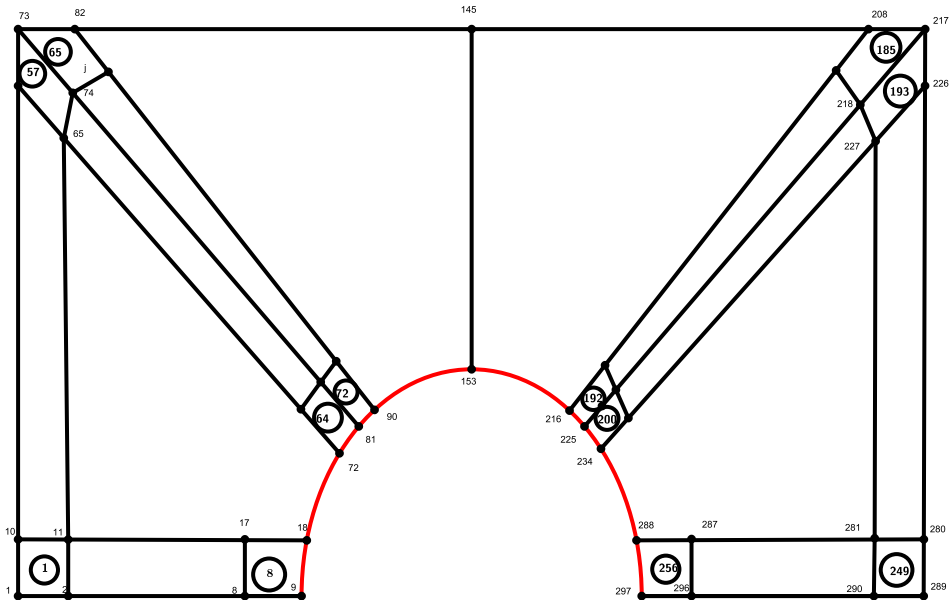

Figure 5: Descretization and Node Numbering for Domain with Semi-Ellipse

Connectivity and Assembly of Elements

The integrals we have developed above are over a typical element. In order to populate (assemble) our global matrix we will use the continuity of the primary variable and balance our secondary variables. Consider two squares that are connected on one side and numbered in a typical manner.

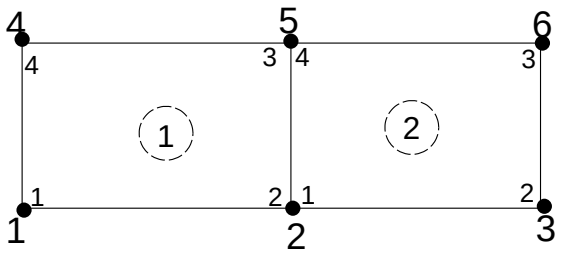

Figure 6: Typical Element and Global Node Numbering

We have a correspondence between the two elements of

Elements Number				
1	1	2	5	4
2	2	3	6	5

Table 2: Correspondence between the Global Nodes

The relation between the local and global nodal values is

$$\begin{aligned} u_1^1 &= U_1 \\ u_2^1 + u_1^2 &= U_2 \\ u_2^2 &= U_3 \\ u_4^1 &= U_4 \\ u_3^1 + u_4^2 &= U_5 \\ u_3^2 &= U_6 \end{aligned}$$

When balancing the secondary variables we just need to make sure that at the interface between our two elements that the flux cancels out. So the flux on the side of 2-3 in element 1 and the 4-1 in element 2 must balance

$$Q_2^1 + Q_1^2 = 0, \qquad Q_3^1 + Q_4^2 = 0$$

we use the relation that we stated above and from that we can write out or assembled matrix. The

assembled matrix is

$$\begin{bmatrix} K_{11}^1 & K_{12}^1 & 0 & K_{14}^1 & K_{13}^1 & 0 \\ K_{21}^1 & K_{22}^1 + K_{11}^2 & K_{12}^2 & K_{24}^1 & K_{23}^1 + K_{14}^2 & K_{13}^2 \\ 0 & K_{21}^2 & K_{22}^2 & 0 & K_{24}^2 & K_{23}^2 \\ K_{41}^1 & K_{42}^1 & 0 & K_{44}^1 & K_{43}^1 & 0 \\ K_{31}^1 & K_{32}^1 + K_{41}^2 & K_{42}^2 & K_{34}^1 & K_{33}^1 + K_{44}^2 & K_{43}^2 \\ 0 & K_{31}^2 & K_{32}^2 & 0 & K_{34}^2 & K_{33}^2 \end{bmatrix} \begin{bmatrix} U_1 \\ U_2 \\ U_3 \\ U_4 \\ U_5 \\ U_6 \end{bmatrix} = \begin{bmatrix} F_1^1 \\ F_2^1 + F_1^2 \\ F_2^2 \\ F_4^1 \\ F_3^1 + F_4^2 \\ F_3^2 \end{bmatrix}$$

CHAPTER III

RESULTS AND DISCUSSION

We consider a square cavity of that has a side of length one. This cavity has three stationary walls and the top lid is moving. The boundary conditions are

$$
\begin{aligned}
v_x = U = 0,\ v_y = V = 0, \qquad & x = 0,\ 0 \le y < 1 \\
v_x = U = 0,\ v_y = V = 0, \qquad & y = 0,\ 0 \le x \le 1 \\
v_x = U = 0,\ v_y = V = 0, \qquad & x = 1,\ 0 \le y < 1. \\
v_x = U = 1,\ v_y = V = 0, \qquad & y = 1,\ 0 \le x \le 1.
\end{aligned}
$$

the geometry is shown below

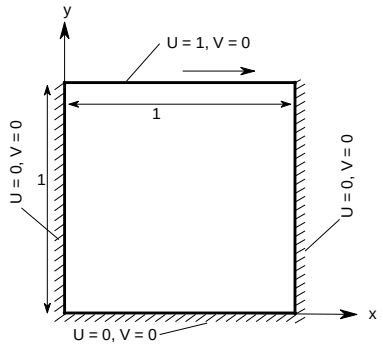

Figure 7: A Rectangular Box with a Moving Lid

Table 3 shows the velocity v_x as a function of y at x=0.5. This result is for a Reynold number of zero .

Y	U
0.0	0.0
0.0625	-0.036882002
0.125	-0.066308714
0.1875	-0.09197926
0.25	-0.11592754
0.3125	-0.13886246
0.375	-0.16027676
0.4375	-0.17819817
0.5	-0.18894558
0.5625	-0.18652318
0.625	-0.1625019
0.6875	-0.10571778
0.75	-0.0038229625
0.78125	0.06819768
0.8125	0.15525836
0.84375	0.25964874
0.875	0.37823987
0.90625	0.5161597
0.9375	0.66410124
0.96875	0.8283758
1.0	1.0

Table 3: Horizontal Velocity Reynold number 0

Figure 8 shows the velocity v_x as a function of y at x=0.5. The blue solid line represents a the horizontal velocity with respect to the y at a Reynolds number of zero. The red dashed line represents the same but with a Reynolds number of 800. As illustrated by the graph, the horizontal velocity behaves differently for different Reynolds numbers. For Reynold number zero the graph is smoother

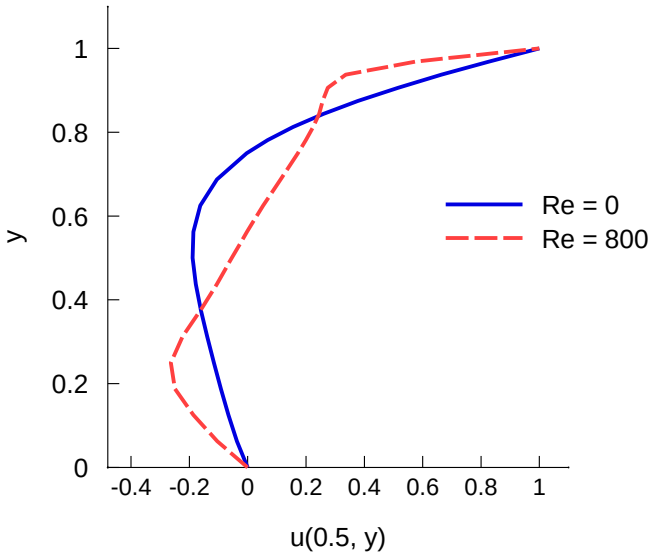

Figure 8: Horizontal Velocity as a Function of y

This figure illustrates how the horizontal velocity behaves for different values of x and y. Notice how the horizontal velocity is negative around y=0.5 and x=0.5.

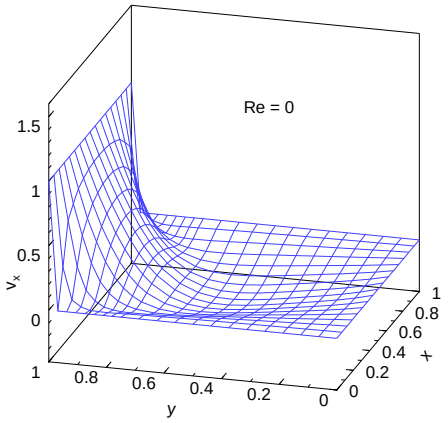

Figure 9: Horizontal Velocity Reynolds Number of Zero

The graph below depicts the vertical velocity for different values of x and y at a Reynolds number of zero.

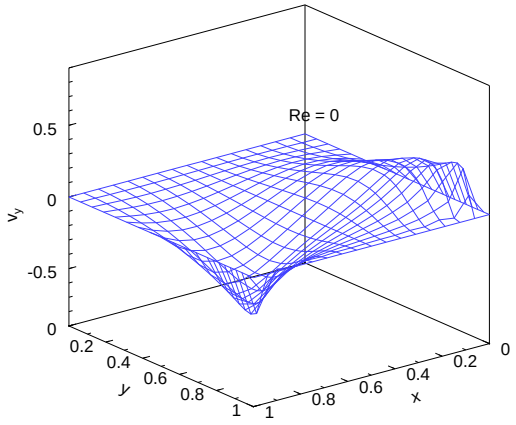

Figure 10: Vertical Velocity Reynolds Number of Zero

In figure 11 the steady state behavior of the flow for a Reynolds number of 0 is shown.

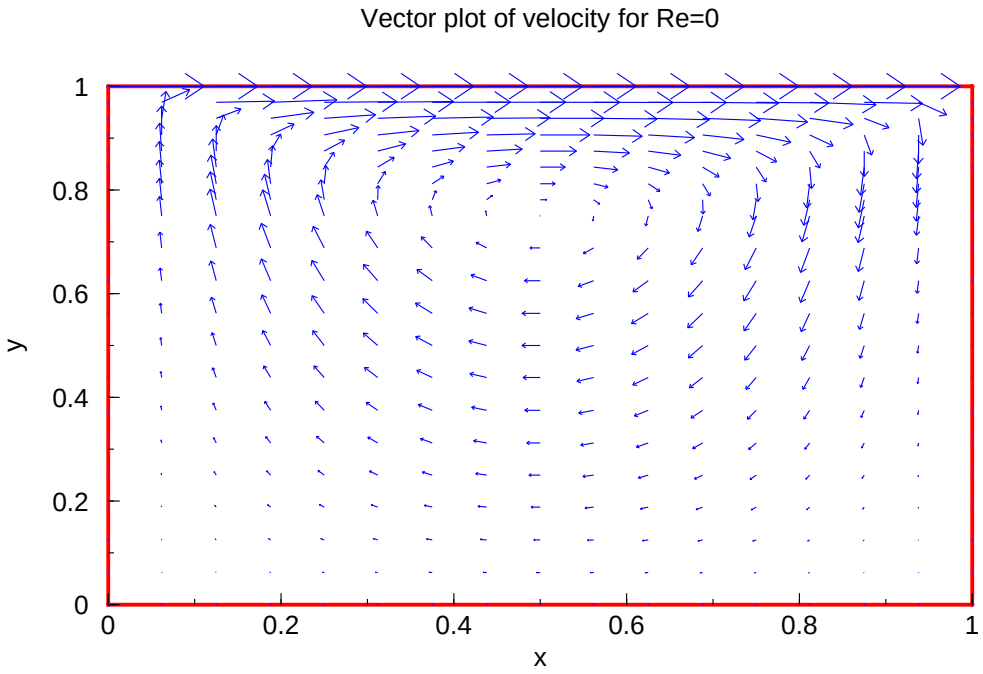

Figure 11: Velocity Plot Reynolds Number of Zero

For a Reynolds number of 800 there is a noticeable difference in the steady state behavior of the graph.

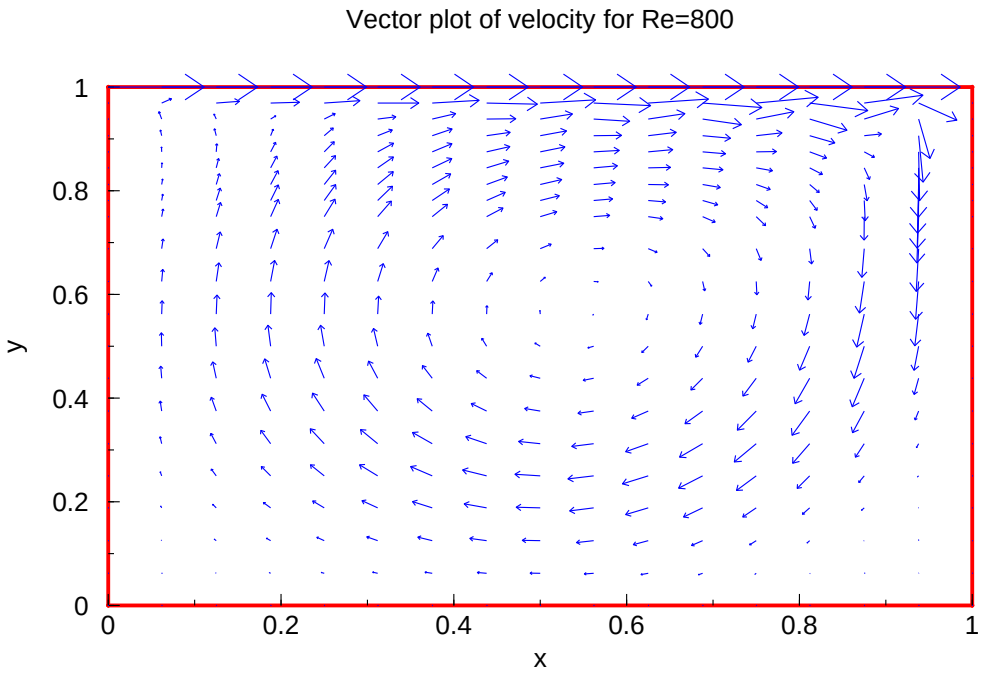

Figure 12: Velocity Plot Reynolds Number of 800

Next, we'll consider a cavity similar to the one above however on the bottom there is a semi-elliptical bump protruding from the bottom up. Below we see the vector plot for a Reynolds number of 0.

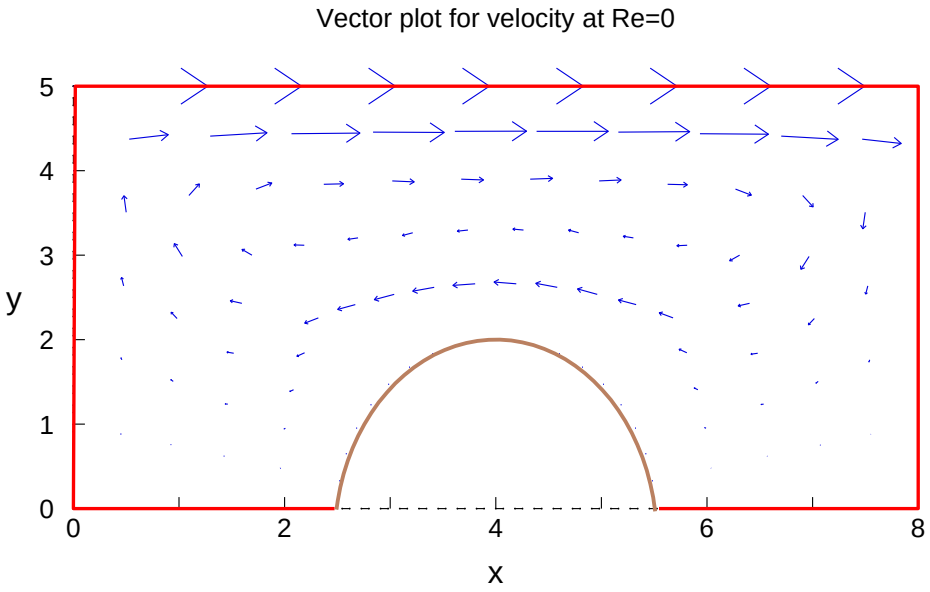

Figure 13: Vector Plot Semi-Ellipse Re=0

In this plot we see flow with Reynolds number of 100.

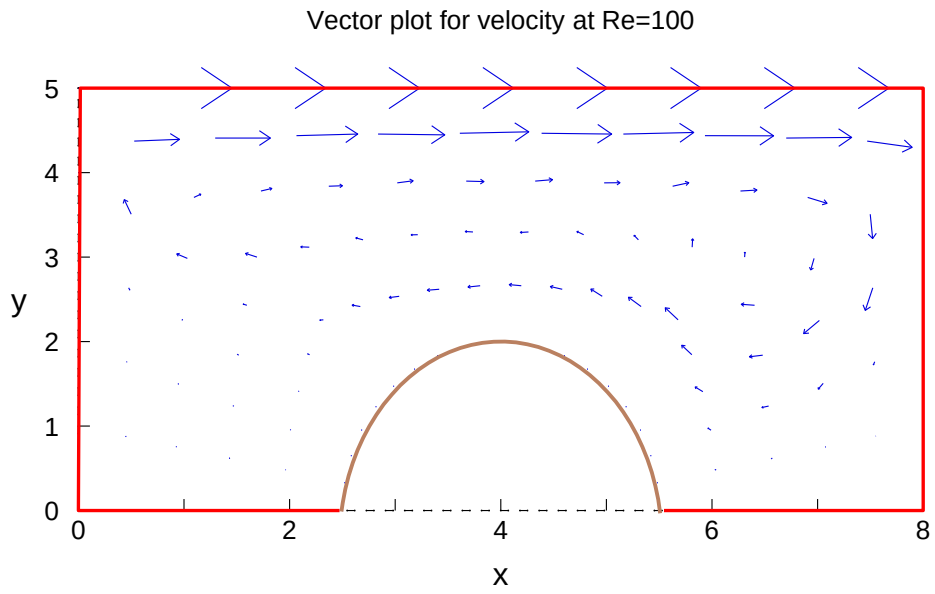

Figure 14: Vector Plot Semi-Ellipse Re=100

The plot below we see now for a Reynolds number of 300.

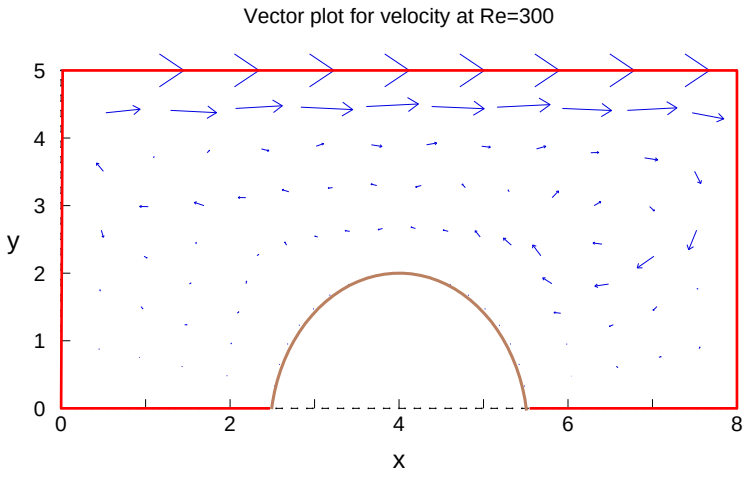

Figure 15: Vector Plot Semi-Ellipse Re=300

Finally for a Reynolds number of 800 we do see a little difference between this plot and the previous one.

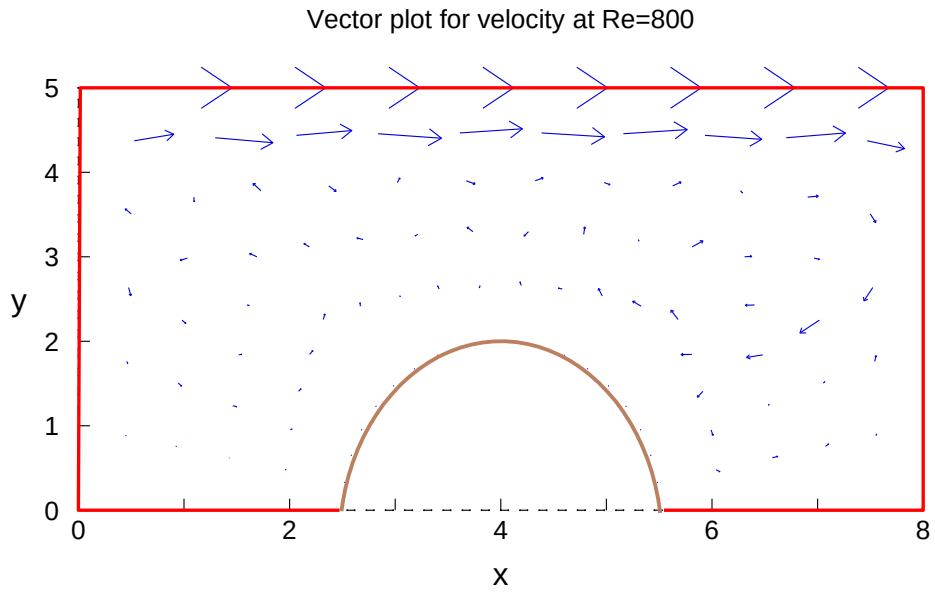

Figure 16: Vector Plot Semi-Ellipse Re=800

Now we increase the node numbers and once again look at the horizontal velocity as a function of y. The blue line is the Reynolds number of zero and the blue dashed line is the Reynolds number 800

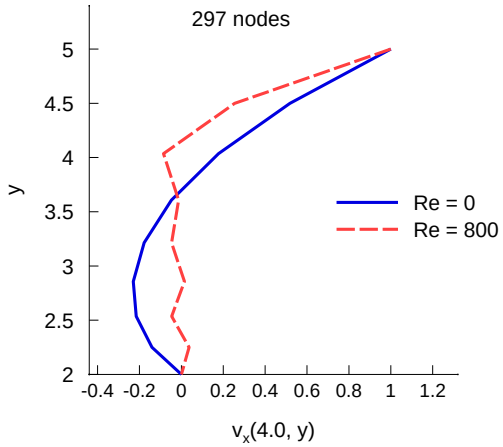

Figure 17: Horizontal Velocity 297 Nodes

In Figure 18 below we observe that the vertical velocity as a function of y with 297 nodes and two different Reynolds numbers. Once again the blue line is the Reynolds number of zero and the blue dashed line is the Reynolds number 800. We observe that the verticle velocity component is zero for a Reynolds number of 800.

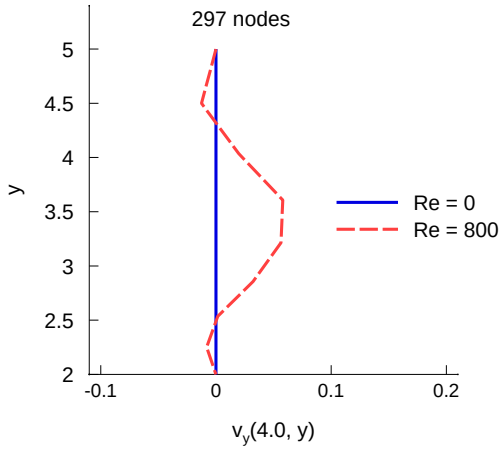

Figure 18: Vertical Velocity 297 Nodes

The vector plot for a Reynolds number of 0 and 297 nodes is depicted below. Notice the details in the behavior of the flow compared to the previous plots. At x=4 the verticle compenent is zero the horizontal compenent is positive at the top part and negative around the bump for a Reynold number of zero.

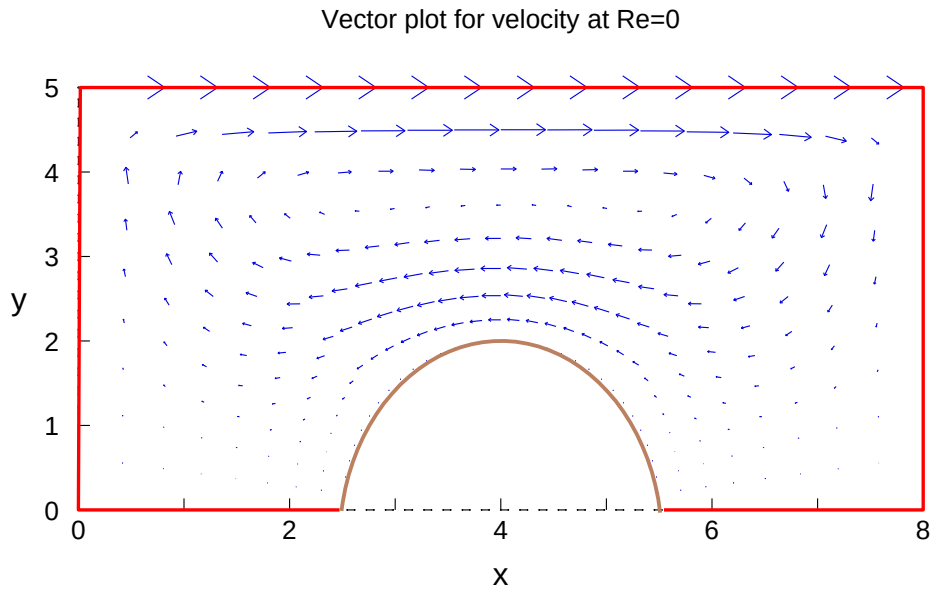

Figure 19: Vector Plot 297 Nodes with Re=0

The vector plot for a Reynolds number of 100.

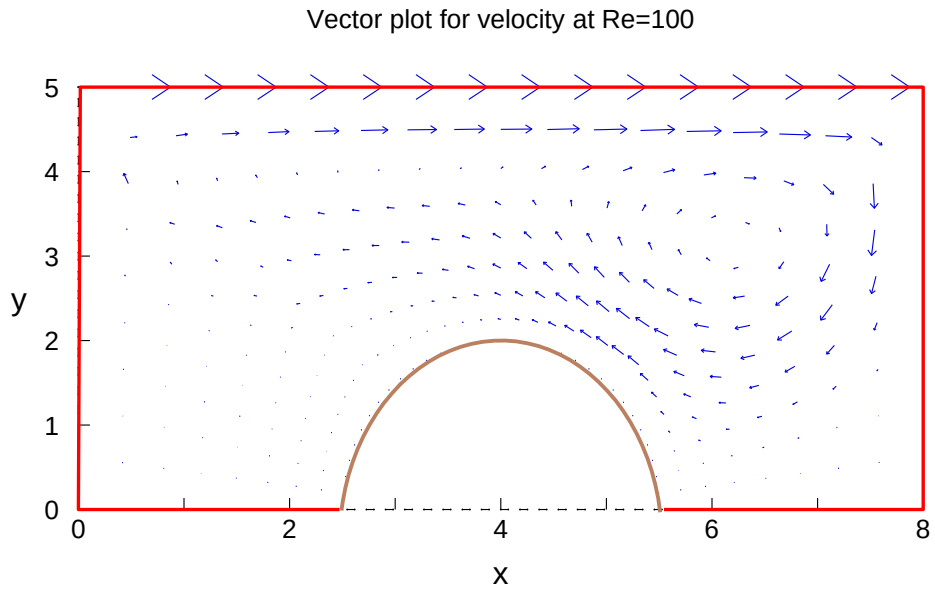

Figure 20: Vector Plot 297 Nodes with Re=100

For a Reynolds number of 300.

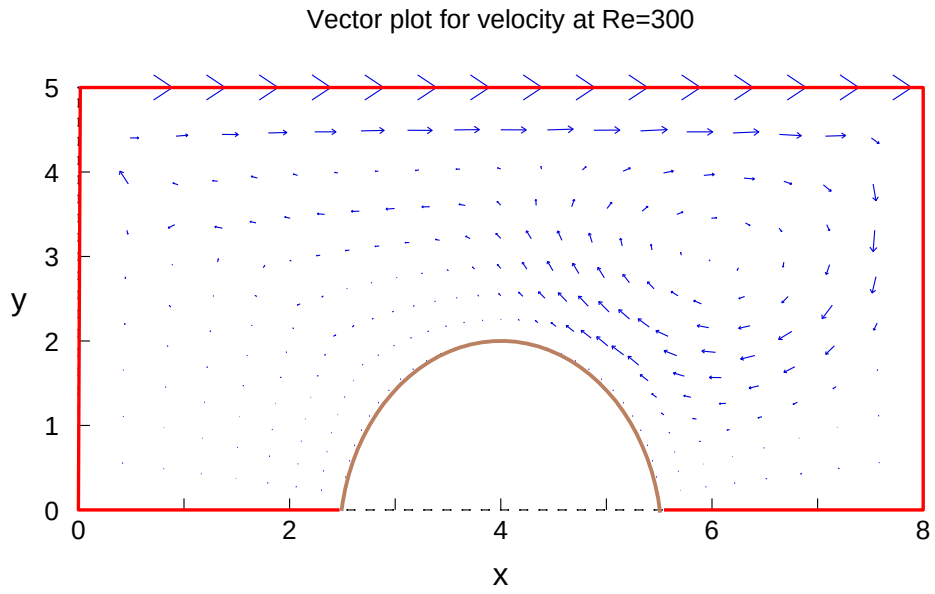

Figure 21: Vector Plot 297 Nodes with Re=300

Now finally for a Reynolds number of 800.

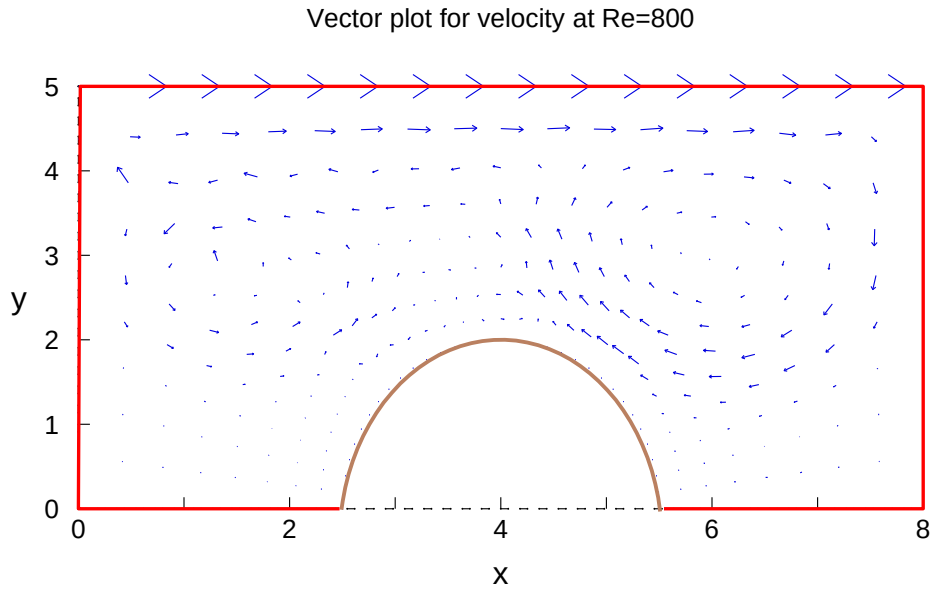

Figure 22: Vector Plot 297 Nodes with Re=800

It has been observed for the square that the horizontal velocity component v_x towards the top is positive while the horizontal velocity towards the bottom is negative. For a Reynold number of zero the the flow is elliptical, and for higher reynolds number both components become dominant and generate circular motion. For the flow with the semi-ellipse the top part is dominated by the horizontal velocity and is moving in the direction of the lid. When the Reynold number was zero the motion in the center was almost parallel.As the Reynold number increases we observe two circular motion on both sides. The motion on the right hand side is more prominent than that of the left. Furthermore the velocity effect is minimal as you approach the stationary sides and becomes zero at the wall.

Conclusion

We considered a cavity filled with fluid whose three sides are stationary with a lid at the top that is moving at a constant speed. We obtained the weak form of the governing equations, and developed the Galerkin finite element method for the steady state case. The Gaussian quadrature method was used to evaluate our integrals. We observed in the case of the square cavity that the horizontal velocity component dominates at the top, and there is uniform flow for a Reynolds number of zero. When the Reynolds number increased the affect of the verticle velocity component is observed throughout the fluid domain. In the case of the cavity with a bump increased Reynold number we observed the flow dominates on the right hand side of the cavity.

REFERENCES

Reddy, J.N. (2005) An Introduction to the Finite Element Method 532-551

Reddy, J.N. (2004) An Introduction to Nonlinear Finite Element Analysis 229-267

Olek C Zienkiewicz, R.L. Taylor, J.Z. Zhu (2005) The Finite Element Method It's Basis and Fundamentals

Reddy, J.N. (1979) On the Finite Element Method with Penalty for Incompressible Fluid Flow Problems, The Mathematics of Finite Elements and Applications II

Kwon, Young W., Bang, Hychoong (1997) The Finite Element using MATLAB

Gockenbach, Mark S., (2006) Understanding and Implementing the Finite Element Method

Ochsner Andreas, Merkel, Markus (2012) One-Dimensional Finite Elements: An Introduction to the FE Method

BIOGRAPHICAL SKETCH

Daniel Montez, born April 9, 1986, grew up in Harlingen, Tx, attending Harlingen High school graduating in 2004. He attended South Texas College earning an Associates of Science in Mathematics in 2010. Later he transferred to the University of Texas-Pan American where he graduated magna cum laude in 2012 with a Bachelors of Science in Applied Mathematics. He went on to earn his Masters of Science in Applied Mathematics from the University of Texas-Pan American in 2013. Professionally he served as a tutor, and later a graduate teaching assistant. While there he was an active member in the Society for Industrial and Applied Mathematics. His permenant mailing address is 3610 Times Square, Harlingen, Tx, 78552.